Published in final edited form as:

Dev Biol. 2020 August 15; 464(2): 176–187. doi:10.1016/j.ydbio.2020.05.008.

The core SWI/SNF catalytic subunit Brg1 regulates nephron progenitor cell proliferation and differentiation

Jeannine M. Basta[a,1], **Ajeet P. Singh**[b,1], **Lynn Robbins**[a,d], **Lisa Stout**[a], **Michelle Pherson**[c], **Michael Rauchman**[a,d,e,*]

[a]John T. Milliken Department of Medicine, Division of Nephrology, Washington University School of Medicine, St. Louis, Mo 63110 USA

[b]Division of Pediatric Hematology/Oncology, Departement of Pediatrics and Department of Biochemistry & Molecular Biology, Pennsylvania State University, Hershey, PA 17033 USA

[c]Department of Biochemistry & Molecular Biology, Saint Louis University, St. Louis, MO 63104 USA

[d]VA St. Louis Health Care System, John Cochran Division, St. Louis, MO, 63106, USA

[e]Deaprtememt of Developmental Biology, Washington University School of Medicine, St. Louis, MO 63110 USA

Abstract

Chromatin-remodeling complexes play critical roles in establishing gene expression patterns in response to developmental signals. How these epigenetic regulators determine the fate of progenitor cells during development of specific organs is not well understood. We found that genetic deletion of *Brg1* (*Smarca4*), the core enzymatic protein in SWI/SNF, in nephron progenitor cells leads to severe renal hypoplasia. Nephron progenitor cells were depleted in *Six2*-Cre, $Brg1^{flx/flx}$ mice due to reduced cell proliferation. This defect in self-renewal, together with impaired differentiation resulted in a profound nephron deficit in *Brg1* mutant kidneys. Sall1, a transcription factor that is required for expansion and maintenance of nephron progenitors, associates with SWI/SNF. Brg1 and Sall1 bind promoters of many progenitor cell genes and regulate expression of key targets that promote their proliferation.

1. Introduction

Formation of a normal complement of nephrons in the mammalian kidney requires expansion and maintenance of self-renewing nephron progenitor cells during embryonic development. After cessation of nephrogenesis, which occurs at birth in humans and post-natal day 4 in mice, no new nephrons form (Hartman et al., 2007; Rumballe et al., 2011). Genetic ablation of nephron progenitor cells by targeting Diphtheria toxin to Six2+ cells in

*Corresponding author. MDCM, Division of Nephrology, Washington University School of Medicine, USA., mrauchma@wustl.edu (M. Rauchman).

[1]These authors contributed equally to this work.

Appendix A. Supplementary data

Supplementary data to this article can be found online at https://doi.org/10.1016/j.ydbio.2020.05.008.

developing kidney leads to a deficit of nephrons at birth (Cebrian et al., 2014). Similarly, deletion or reduction of expression of genes that are required for proliferation of nephron precursors or to prevent their loss by apoptosis lead to a reduction in nephron endowment (Couillard and Trudel, 2009; Denner and Rauchman, 2013; Blank et al., 2009; Brown et al., 2011, 2015; Muthukrishnan et al., 2015). These studies establish that maintenance of the nephron progenitor pool determines nephron endowment. There appears to be no mechanisms that sense nephron number during development that can compensate for a reduction in the pool of progenitors to restore the number of nephrons to the normal range. Moderate reductions in nephron number at birth due to intra-uterine growth retardation or prematurity is associated with hypertension and chronic kidney disease in adulthood (Barker et al., 2000; Hoy et al., 2006; Keller et al., 2003). More severe reductions in nephron endowment, termed congenital renal hypoplasia, is a common cause of childhood renal failure.

Epigenetic modifications of chromatin play an essential role in regulating gene expression in developing organs. These include enzymatic activities that mediate DNA methylation, ATPases that slide or evict nucleosomes and enzymes that modify lysine tails of histones. These modifications increase or restrict access of DNA binding factors and the transcriptional machinery to DNA to regulate the level of gene expression in a temporal and spatial manner. Multi-protein complexes that modify chromatin associate with transcription factor networks that control progenitor cell fate, cell lineage and terminal differentiation. Genetic mutations that affect epigenetic modifiers highlight their importance in kidney development. Mutations in Chromodomain-Helicase-DNA binding protein (*CHD7*), an ATP dependent chromatin remodeler in the Tri-thorax family, cause CHARGE syndrome, which is often associated with renal hypoplasia (Legendre et al., 2017). Rubinstein-Taybi syndrome, in which kidney developmental defects also feature prominently, is due to mutations in genes encoding the histone acetylase CBP/p300 (Fergelot et al., 2016). Genetic deletion of DNA methyltransferase 1 (*Dnmt1*) in Six2+ cells leads to renal hypoplasia due to reduced proliferation of progenitor cells and ectopic expression of germline genes that would normally be repressed in developing kidney (Li et al., 2019; Wanner et al., 2019). *Eed*, a unique subunit of Polycomb repressive complex 2 (PRC2) is required to maintain nephron progenitor cells and promote their differentiation (Zhang et al., 2018). Loss of function of *Chd4*, the ATPase for the nucleosome remodeling and deacetylase (NuRD) chromatin-remodeling complex, results in renal hypoplasia due to the inability to maintain Six2+ nephron progenitors (Denner and Rauchman, 2013).

These studies establish an important role for epigenetic modifiers in developing kidney. However, the mechanisms by which they control progenitor cell fate in specific organs is not well understood. Chromatin remodeling complexes regulate developmental gene expression by their association and functional cooperativity with transcription factors. *Pax2*, an essential gene in human and mouse kidney development, can activate or repress gene expression. Elegant studies from Patel et al. showed that Grg4 displaces PTIP and the H3K4 methylation complex, thereby preventing Pax2-mediated gene activation (Patel et al., 2012). Grg4 silences genes with Pax2 DNA binding sites by recruitment of the Polycomb repressive complex. Sall1, another gene that is indispensable for proper kidney development in humans and mice, associates with the Nucleosome Remodeling and Deacetylase Complex (NuRD).

Disruption of Sall1-NuRD interaction in knock-in mice (*ΔSRM*) leads to depletion of nephron progenitor cells due to their unrestrained differentiation and premature cessation of nephrogenesis (Basta et al., 2017). De-repression of differentiation genes, such as *Pax8* and non-canonical *Wnt* signaling genes, is thought to be an important mechanism contributing to ectopic differentiation in *Sall1* mutants (Basta et al., 2014, 2017). These results suggested a model whereby Sall1 cooperates with NuRD to inhibit expression of differentiation genes and allow self-renewal of nephron progenitors to proceed, which enables a normal complement of nephrons to form. However, comparing the phenotypes of *ΔSRM* and *Sall1* null mutant mice revealed that *Sall1* also regulates proliferation of nephron progenitors, independently of NuRD (Basta et al., 2014, 2017).

We hypothesized that Sall1 interacts with other chromatin-remodeling factors to regulate proliferation of nephron progenitor cells. Using an unbiased proximity proteomics screen for Sall1 interacting proteins, we identified multiple components of the SWItch-Sucrose Non-Fermentable (SWI/SNF) chromatin-remodeling complex (Bozal-Basterra et al., 2018). SWI/SNF is an important regulator of the cell cycle in developing and neoplastic tissues (Nagarajan et al., 2020; Ruijtenberg and van den Heuvel, 2015; Stojanova et al., 2016). While the SWI/SNF complex has important roles in embryonic development in multiple tissues, including ES cells, early embryogenesis, heart and CNS [reviewed in (Hota and Bruneau, 2016)], its function in developing kidney is poorly understood. In this report, we demonstrated that genetic deletion of *Brg1* (*Smarca4*), the catalytic subunit of SWI/SNF in Six2+ cells led to profound growth retardation and nephron deficit. Brg1 is required for expansion and maintenance of nephron progenitor cells. Sall1 and Brg1 were enriched at the promoters of many progenitor genes and regulate the expression of *Bmp7*, *Fgf9* and *Myc*, key targets that regulate proliferation of nephron progenitor cells. We found that Brg1 was also required to promote progenitor cell differentiation. These studies identify pleiotropic effects of SWI/SNF to promote kidney growth and nephron formation.

2. Materials and methods

2.1. Protein interaction assays

GST-Sall1 wild type and Sall1-ΔSRM fusion proteins were cloned into pEBG and expressed in COS-1 cells (ATCC CRL-1650). After 48 h, cells were lysed, and precipitated with glutathione sepharose, as described (Basta et al., 2017). Lysates were analyzed by western blot using primary and HRP labeled secondary antibodies (Table S1) to detect endogenous subunits of NuRD (Mta2, RbAp48), SWI/SNF (Brg1, Smarcc1/BAF155), GST and GAPDH (loading control).

2.2. Mice

All animal studies were carried out in accordance with the guidance of the Institutional Animal Use and Care Committee of Washington University School of Medicine. *Brg1* floxed/floxed mice (B6; 128S2-Smarca4^{tm1Pcn}/Mmnc) were a generous gift from Trevor Archer [NIEHS, Research Triangle Park. North Carolina (Singh et al., 2016),]. To generate the inducible Cre-Brg1flox/flox mice, Brg1flox/flox mice were bred with *Six2*-TGC BAC transgenic mice that express Cre recombinase in the Six2+ nephron progenitor cells

[(Kobayashi et al., 2008), Jackson Labs #009606]. The deleted Brg1flox/flox allele does not produce a functional protein. For genotyping, genomic DNA was amplified with the following oligonucleotide primers: 5′-GTCATACTTATGTCATAGCC-3′ and 5′-GCCTTGTCTCAAACTGATAAG-3'.

2.3. Immunofluorescence

Embryonic kidneys were fixed with 4% PFA overnight, submerged in 20% sucrose in PBS and embedded in OCT. 10 μm frozen sections were washed with cold 100% MeOH, boiled in 10 mM citric acid pH 6 for 20 min, and incubated with primary antibodies (Table S1). Reactivity was detected using fluorescently labeled secondary antibodies (Table S1). Sections were counter stained with DAPI (Sigma Aldrich), mounted in Mowiol 4–88 (Poly Sciences, Inc.), and digital images acquired using a Nikon 80i epifluorescence microscope with a Retiga R3 camera and a Leica DM5000B epifluorescence microscope with a Leica DFC365FX camera.

2.4. Quantification of Six2 positive caps, Cytokeratin + Ub tips, renal vesicles and terminally differentiating nephron segments

Embryonic day 14.5, 16.5 and 17.5 kidneys were immunostained for Six2, Cytokeratin and DAPI. Six2+ caps and Cytokeratin + UB tips were counted from at least 10 non-sequential sections (10× magnification) from at least 3 independent embryos for each stage and genotype. Results were reported as the average number of caps or UB tips per high-powered field (HPF) ± s.e.m. For renal vesicles, embryonic day 14.5 and 16.5 kidneys were immunostained for NCAM and Lef1. For terminal nephron segments, immunostaining was performed to detect Wt1 (glomeruli), Megalin (proximal tubule), NKCC2 (loop of Henle), NCC (distal tubule) and cytokeratin (collecting duct). All structure quantification was performed by counting positive staining for cross sections of tubules, eg for proximal tubules multiple cross-sections of the same tubule may have been counted, however counting was performed consistently for both control and mutant samples. Structures were counted on at least ten non-sequential sections (10 × magnification) from at least three independent embryos for each genotype.

2.5. Mitosis and apoptosis of Six2 positive cells

Mitosis was determined by staining embryonic kidneys (E14.5, 16.5, 17.5) for pHH3 and Six2. Nuclei were stained using DAPI. The total number of pHH3 and Six2/pHH3+ cells were counted on at least 12 non-sequential sections (10× magnification) from at least three independent embryos for each stage and genotype. Apoptosis was determined by performing TUNEL analysis using the ApopTag Red *In Situ* Apoptosis Detection Kit (Millipore). The total number of TUNEL and Six2/TUNEL + cells were counted on at least 16 non-sequential sections (10 × magnification) from 4 independent embryos for each stage (E14.5 and 16.5) and genotype. Results are reported as the average # of cells/HPF ± s.e.m.

2.6. RNA-sequencing (RNA-seq)

Total RNA was isolated from three E17.5 kidneys for each genotype using an RNeasy Mini Kit (Qiagen 74104) with on the column DNAse I treatment. Ribosomal RNA was depleted

from 1 μg of total RNA using Ribominus Eukaryote System v2 (Life Technologies). Construction of barcoded sequencing libraries was performed using the Ion Total RNA-seq v2 kits (Life Technologies) according to the manufacturer's instructions. Sequencing was performed on an Ion Torrent Proton with mean read lengths of 110–170 nucleotides, and reads were aligned to the mouse mm10 genome using the TMAP aligner map4 algorithm. Soft-clipping at both 5′ and 3′ ends of the reads was permitted during alignment to accommodate spliced reads, with a minimum seed length of 20 nt. Genome-wide strand-specific nucleotide coverages were calculated from the aligned bam files for each sample using the *genomecoveragebed* program in BEDTools (Quinlan and Hall, 2010) and the nucleotide coverage for all non-redundant exons for each gene were summed using custom R scripts (R Core Team, 2015; http://www.R-project.org). Normalization factors were calculated by averaging the total exon coverage for all replicates and dividing this average by the total exon coverage for each individual sample. The total coverage for each gene in each replicate was then multiplied by these factors after adding an offset of 1 to each gene to preclude division by 0 in subsequent calculations. The averages and p values of the coverage values for all genes in the individual groups were calculated using Microsoft Office Excel. The expression values for each gene are the normalized strand-specific total nucleotide coverage for each gene.

2.7. Quantitative real-time PCR (qRT-PCR)

Total RNA was isolated from embryonic kidney tissue using an RNeasy Mini Kit with DNAse I treatment on the column (Qiagen). cDNA was prepared using the High Capacity RNA-to-cDNA kit (Life Technologies). Primer sequences are in Table S2 qRT-PCR was performed using a Quant Studio 3 (Applied Biosystems) Thermocycler and SYBR Green PCR Master Mix (Life Technologies) as described previously (Kiefer et al., 2012). Real-time reactions were performed in triplicate and relative expression was calculated using the delta CT method and normalized to *Gapdh* or *Hprt1* control transcripts (Kiefer et al., 2012).

2.8. Chromatin immunoprecipitation sequencing (Chip-seq)

E16.5 kidneys were isolated in PBS + Ca and Mg on ice and crosslinked. For Sall1 and H3K27ac ChIP kidneys were crosslinked with 2 mM Di (N succinimidyl) glutarate (DSG, Proteo Chem C1104) in PBS for 30 min with rocking at room temperature followed by the addition of 1% formaldehyde (Thermo Scientific 28906) and incubation for an additional 10 min with rocking at room temperature. For Brg1, RNA Pol2 Ser2 and H3K4me1 ChIP, kidneys were crosslinked with 1% formaldehyde for 30 min with rocking at room temperature. Crosslinking was quenched with 125 mM glycine for 5 min at room temperature and kidneys were washed three times with PBS with protease inhibitors and flash frozen on dry ice. Kidneys were homogenized with a hand held dounce homogenizer in Lysis Buffer 1 (50 mM HEPES-KOH pH 7.5, 140 mM NaCl, 1 mM EDTA, 10% glycerol, 0.5% NP-40, 0.25% Triton-X 100) and incubated for 20 min at 4 °C with rocking. Samples were pelleted at 2800 rpm at 4 °C for 5 min and the supernatant discarded. Pellets were resuspended in Lysis Buffer 2 (10 mM Tris-HCl pH 8.0, 200 mM NaCl, 1 mM EDTA, 0.5 mM EGTA), briefly homogenized and rocked gently for 10 min at room temperature. Nuclei were pelleted at 2800 rpm for 5 min at 4 °C and resuspended in Lysis Buffer 3 (10 mM Tris-HCl pH 8.0, 100 mM NaCl, 1 mM EDTA, 0.5 mM EGTA, 0.1% Na-Deoxycholate, 0.5% N-

lauroylsarcosine). Chromatin was sheared to a size of 100–1000bp using a Covaris ME220. 100 μg chromatin was pre-cleared with 20 μl protein A/G magnetic beads (Thermofisher Scientific 88803) for 2 h rocking at 4 °C. Pre-cleared chromatin was incubated with primary antibody (Table S1) overnight with rocking at 4 °C. The next morning 25 μl protein A/G magnetic beads were added and incubated for 4 h at 4 °C. Complexes were washed 5 times with cold modified RIPA buffer (50 mM HEPES-KOH pH 7.5, 500 mM LiCl, 1 mM EDTA, 1% NP-40, 0.7% Na-Deoxycholate) and 2 times with TE (10 mM Tris pH 8.0, 1 mM EDTA). Complexes were eluted by incubating at 65 °C for 30 min in Elution Buffer (50 mM Tris, 10 mM EDTA, 1% SDS). Crosslinks were reversed by adding NaCl (0.2 M) and heating at 65 °C for 15 h, 200 μg/mL RNase A was added and incubated for 2 h at 37 °C, and 200 mg/mL Proteinase K added and incubated 2 h at 63 °C. DNA was isolated using the MinElute PCR Purification Kit (Qiagen 28004). 2 ng DNA was sheared to 100–300 bp and sequencing libraries were constructed using the Ion Plus Fragment Library Kit (Thermofisher Scientific 4471269) according to (Dorsett and Misulovin, 2017). ChIP-seq and input libraries were sequenced on an Ion Torrent Proton to approximately 2-fold and 12-fold genome coverage, respectively. Reads were aligned to the mm10 mouse genome using the TMAP aligner map4 algorithm. Genome coverage was calculated for ChIP and input samples using BedTools. ChIP sample coverage was normalized to input coverage and ChIP enrichment bedgraphs were generated using described methods (Dorsett and Misulovin, 2017). ChIP peaks were defined as regions of ChIP enrichment in the 99th percentile or greater across a genomic region spanning 300 bp or more. Called peaks were assigned to genomic features (promoters, enhancers) using Bedtools based on peak overlap or falling within a 500 bp window of the defined feature. Remaining peaks were assigned to gene bodies or intergenic regions based on peak overlap with annotated gene regions. Genomic features were defined using published ENCODE datasets for H3K4me3 (GSE83044), H3K27ac (GSE82636), H3K27me3 (GSE82821), and ATAC-seq [ENCSR732OTZ] and the H3K4me1 data from this study. Active promoters were defined as 1000 bp regions of H3K4me3 enrichment overlapping the first exon of an annotated gene and centered on an overlapping ATAC-seq peak when present. If no ATAC-seq peak was present, the region was centered on the annotated transcription start site. Predicted active enhancers were defined as 1000 bp regions of overlapping H3K27Ac and H3K4me1 centered on an ATAC-seq peak and not overlapping an active promoter. ChIP-seq was performed in triplicate for Sall1, duplicate for Brg1 and one independent sample for RNA Polymerase and histone modifications. Gene Ontology analysis was performed using DAVID Gene ontology analysis (Huang et al., 2009a, 2009b) and Geneontology.org (Ashburner et al., 2000; The Gene Ontology, 2019). Venn diagrams were generated using Venny 2.1 (Oliveros, 2007).

2.9. Statistical analysis

Data are presented as the mean ± SEM. We calculated statistical significance using a two-tailed Student's t-test or a one-way ANOVA followed by multiple-group comparison analysis with Tukey correction. We considered differences with a p value of 0.05 or less to be statistically significant.

3. Results

3.1. Sall1 associates with components of the SWI-SNF complex

We previously demonstrated that homozygous deletion of *Sall1* leads to profound depletion of Six2+ nephron progenitor cells due to both unrestrained differentiation and reduced proliferation (Basta et al., 2014; Kanda et al., 2014). Disrupting the interaction between Sall1 and the nucleosome remodeling and deacetylase (NuRD) complex in knock-in mice resulted in premature differentiation of nephron progenitors, but had no effect on their proliferation (Basta et al., 2017), suggesting that Sall1 associates with other co-factors to regulate cell cycle progression in these cells. An unbiased proteomics screen for Sall1 interacting proteins identified several candidates that could cooperate with Sall1 to control cell proliferation (Bozal-Basterra et al., 2018). Among the most promising candidates, we focused on the SWItch-Sucrose Non--Fermentable (SWI/SNF) chromatin-remodeling complex because of its well-described role in regulating cell proliferation in developing tissues and renal carcinoma, and in maintaining naïve pluripotency of ES cells (Singh et al., 2016, 2017; Gatchalian et al., 2018; Porter and Dykhuizen, 2017). We hypothesized that Sall1 associated with SWI/SNF to regulate self-renewal of nephron progenitor cells.

To validate the results obtained with the proteomics screen, we tested for association of Sall1 with two core SWI/SNF components, Brg1 (*Smarca4*) and Baf155 (*Smarcc1*). COS-1 cells were transfected with a vector expressing a GST-Sall1 fusion protein. Cell lysates precipitated with glutathione sepharose beads (GST) were analyzed by western blot. Sall1 associated with endogenously expressed Brg1 and Baf155 (Fig. 1). Sall1 interacts with the NuRD chromatin-remodeling complex via a 12 amino acid N-terminal motif in Sall1 designated as the Sall1 Repression Motif (SRM) (Lauberth et al., 2007; Lauberth and Rauchman, 2006). As expected, mutations in basic amino acid residues of the SRM abrogated interaction with NuRD components Mta2 and RbAp48. However, the Sall1-ΔSRM mutation did not disrupt the interaction between Sall1 and the SWI/SNF components Brg1 and Baf155. We conclude that Sall1 associates with SWI/SNF through a domain that is distinct from the region that mediates Sall1-NuRD interaction.

3.2. Differential expression of SWI/SNF complex subunits in developing kidney

In mammals, there are two main subtypes of SWI/SNF, BAF and PBAF, which contain identical core components, paralogs, and unique proteins that distinguish between these complexes [reviewed in (Bracken et al., 2019)]. Recently, a third subtype termed non-canonical BAF was identified (Fig. 2A). To begin to define the role of SWI/SNF in kidney development, we evaluated the temporal expression pattern of its subunits in developing kidney (Fig. 2B). Based on this analysis we classified SWI/SNF complex components into three expression patterns. We identified one subgroup that included genes encoding Brg1 (*Smarca4*), Baf200 (*Arid2*), Baf180 (*Pbrm1*), *Smarcd1/2/3* (Baf60a/b/c), Baf47 (*Smarcb1*), Baf45a (*Phf10*), Baf45 d (*Dpf2*) and *Brd7* expressed at similar levels through different stages of the developing kidney (Fig. 2B). Expression in the second subgroup peaked at earlier stages of nephrogenesis (E12.5–15.5). This expression pattern was evident for the BAF specific subunit complex Baf250a (*Arid1a*), and for Baf155 (*Smarcc1*), Baf57 (*Smarce1*) and Baf53a (*Actl6a*), which are components of both the BAF and PBAF

complexes (Fig. 2A). The last subgroup consisting of Baf250b (*Arid1b*) and Baf170 (*Smarcc2*) demonstrated increased expression at late stage kidney formation and near termination of nephrogenesis (E17.5-P2). These data suggest that some SWI/SNF subunits undergo developmental switching during kidney development. Some subunit isoforms were not detected (*Baf53b*, *Baf45b*) or were expressed at very low levels (*Baf45c*) in the kidney. Overall, SWI/SNF expression was greater in the embryonic compared with the adult kidney. Brg1 (*Smarca4*), the catalytic subunit was expressed at similar levels throughout kidney formation and its level declined in the adult kidney. In contrast, Brm (*Smarca2*), the alternative SWI/SNF ATPase was expressed at very low levels throughout development and its level was increased in the adult kidney (Fig. 2B). We conclude that SWI/SNF components of BAF and PBAF are expressed in developing kidney.

3.3. Deletion of Brg1 in nephron progenitor cells results in renal hypoplasia

Because *Smarca4* (Brg1) encodes the ATPase activity essential for the function of SWI/SNF complexes and its expression is preferred over *Smarca2* (Brm) in embryonic kidney, we focused our analysis on this subunit. Brg1 protein was detected in all compartments of the developing kidney including the Six2+ nephron progenitors in the cap mesenchyme (CM), stroma, differentiating nephrons and ureteric bud [UB] (Fig. 3A). To examine the function of *Brg1* in nephron progenitors, *Brg1* was deleted from the Six2+ cap mesenchyme (CM). We crossed *Six2-Cre:GFP* [*Six2GC* (Kobayashi et al., 2008)] to $Brg1^{loxP/loxP}$ to generate $Six2^{GC/+}$; $Brg1^{loxP/loxP}$ mice (hereafter referred to as *Six2Cre*; $Brg1^{flx/flx}$) to delete *Brg1* in CM. Immunostaining confirmed loss of expression of Brg1 in CM surrounding the UB tips in *Six2Cre*; $Brg1^{flx/flx}$ mutant kidney (Fig. 3A). Expression of Brg1 persisted in the UB and stroma, confirming that *Six2-Cre* specifically deleted *Brg1* in the CM (Fig. 3A). Kidney development proceeded normally until E14.5–15.5 when a minority (~10–20%) of *Brg1* mutant kidneys were reduced in size (Table 1, Fig. 3B). However, after E15.5, growth of the *Brg1* mutant kidney was significantly reduced compared with wild type littermates.

3.4. Reduced proliferation of nephron progenitor cells in Brg1 mutant kidneys

To investigate the cause of renal hypoplasia in the *Brg1* mutant, we quantitated Six2+ caps and cytokeratin positive UB tips at different embryonic stages. The number of UB tips were significantly reduced by 38% in the *Brg1* mutant compared with control littermates at E14.5 and by 44% at E17.5 (Fig. 3C and D), but not at E16.5. There was a significant decrease in the number of Six2+ caps surrounding individual UB tips at each time point examined, E14.5 (40%), E16.5 (25%), and E17.5 (63%) [Fig. 3C, E]. To determine the cause of nephron progenitor cell (NPC) loss in *Brg1* mutants, we measured cell proliferation and apoptosis. The total number of pHH3+ cells as well as the number of pHH3/Six2 double positive cells was significantly diminished in the mutant compared with control littermates at E14.5 (31%), E16.6 (39%) and E17.5 (71%) [Fig. 4A, B, C]. In contrast, we did not find an increased number of Six2+ cells undergoing apoptosis in the mutant determined by TUNEL assay at E14.5 or 16.5 (Fig. 4D, F). Together, these results indicate that reduced proliferation, but not apoptosis caused depletion of NPCs, in *Six2Cre*; $Brg1^{flx/flx}$ kidneys. The marked reduction of NPC proliferation and Six2+ caps at E17.5 is consistent with the profound degree of growth retardation of the kidney that is apparent between E17.5 and P0 (Fig. 3B).

3.5. Apoptosis and impaired formation of developing nephrons in Brg1 mutant kidneys

We found a 2.2-fold increase in the total number of TUNEL positive cells in *Brg1* mutant kidneys at E16.5 compared with control kidneys (Fig. 4D and E). However, as noted above, the increase in apoptosis was not evident when we analyzed Six2/TUNEL double positive cells. Rather, apoptotic cells localized towards the interior of the embryonic kidney in developing nephrons and stroma (Fig. 4D). While this finding indicated that apoptosis contributed to renal hypoplasia in *Brg1* mutants, the degree and timing of nephron loss also suggested formation of nephrons was impaired. We examined nephron induction and segmental differentiation in these mutants. At E14.5, prior to finding increased apoptosis, there was a 50% reduction of Lef1/NCAM + renal vesicles in *Six2Cre*; $Brg1^{flx/flx}$ kidneys compared with $Brg1^{flx/flx}$ control littermates (Fig. 5B). Formation of Wt1+ immature glomeruli and megalin + proximal tubules was readily apparent at E14.5 in control kidneys. In contrast, formation of these proximal nephron segments was markedly diminished in *Brg1* mutants by 50% for Wt1+ developing glomeruli and by 87% for megalin + tubules. At E16.5, the formation of all nephron segments, with the exception of collecting ducts, was reduced by >50% (Fig. 5A, C). Together, these findings indicate that impaired nephron induction contributes significantly to renal hypoplasia in *Six2Cre*; $Brg1^{flx/flx}$ kidneys.

3.6. Brg1 regulates genes that promote expansion and differentiation of NPCs

To identify the molecular basis for the kidney phenotype in *Brg1* mutants, we performed transcriptional profiling of E17.5 $Brg1^{flx/flx}$ and *Six2Cre*; $Brg1^{flx/flx}$ kidneys by RNA-seq. We found 781 genes downregulated in the mutant and 726 upregulated using a cut-off of 2-fold change in expression (Fig. 6A). Consistent with the loss of Six2+ NPCs, multiple genes that regulate the expansion of Six2+ NPCs displayed altered expression in the mutant (Fig. 6B). *Bmp7*, *Myc*, *Fgf9*, *Six2*, genes that are required for proliferation and maintenance of NPCs in a self-renewing state, were significantly downregulated in the mutant kidney (Couillard and Trudel, 2009; Blank et al., 2009; Muthukrishnan et al., 2015; Kobayashi et al., 2008; Barak et al., 2012). *Fat4*, an atypical cadherin that limits expansion of NPCs, and *Cdkn1a*, cell cycle inhibitor, were upregulated in the mutant kidney (Bagherie-Lachidan et al., 2015). We also found altered expression of genes that regulate differentiation of NPCs. Differentiation genes *Lhx1*, *Fgf8*, *Hnf1b*, and *Ccnd1* were downregulated, while *Decorin* (*Dcn*), a secreted factor that inhibits Bmp7-mediated differentiation of NPCs was significantly upregulated (Fetting et al., 2014).

To gain further insight into signaling pathways regulated by Brg1 in developing kidney, we performed gene ontology analysis. Among downregulated genes, several metabolic pathways, including oxidative phosphorylation, were highly enriched (Fig. 6C). Reduction in transport pathways included many genes involved in metabolic processes. Our analysis also revealed that expression of many ribosomal genes was inhibited, suggesting global effects on protein translation. Negative effects of *Brg1* loss on metabolic processes and protein synthesis could account for the profound deficit in growth of the kidney between E17.5 and P0 (Fig. 3B). Among upregulated genes, cell adhesion pathways were dramatically induced (Fig. 6C), similar to gene ontology analysis of genes upregulated in *Sall1*−/− mutant progenitor cells (Basta et al., 2014).

The RNA-seq data identified several genes and molecular pathways that could account for renal hypoplasia in *Brg1* mutant kidneys. To identify the early events that impair nephrogenesis, we examined gene expression at E14.5, before significant renal hypoplasia was evident (Fig. 6D). We tested expression of genes that encode for enzymes in oxidative phosphorylation and that exhibited the greatest reductions in transcript levels. These genes, *Cox5b*, *Cox7b*, *ATP5j2*, which were each reduced ~60% at E17.5, were not downregulated at E14.5. Similarly, ribosomal genes *Rpl12* and *Rpl36*, which were reduced ~68% at E17.5, were not changed at E14.5. In contrast, *Bmp7*, *Fgf9* and *Myc* were significantly downregulated at E14.5 and E17.5. These results indicate that *Bmp7*, *Fgf9* and *Myc*, which function cooperatively to promote proliferation of NPCs (Muthukrishnan et al., 2015) are dependent on *Brg1* for expression in developing kidney. We conclude that reduced expression of these factors significantly contributes to reduced proliferation of NPCs.

We performed ChIP-seq on E16.5 wild type kidney to define genomic binding of Brg1. As shown in the pie chart in Fig. 6E, Brg1 preferentially binds promoters in developing kidney. To identify genes that are likely direct transcriptional targets of Brg1, we compared RNA-seq results with ChIP-seq results. Brg1 binding was enriched at promoters of 626 genes that showed altered expression (315 upregulated, 311 downregulated) in the *Brg1* mutant kidney by RNA-seq (Fig. 6F). The gene expression data (Fig. 6B, D) identified target genes that likely contribute significantly to the kidney phenotype in this mutant. We therefore analyzed these genomic loci for Brg1 binding. Significant binding of Brg1 was detected at promoters for multiple downregulated genes that promote proliferation and maintenance of NPCs, including *Bmp7*, *Fgf9*, *Myc* and *Six2* (Fig. 7D–H). We also detected enrichment for Brg1 at promoters of downregulated differentiation genes, including *Lhx1*, *Fgf8* and *Hnf1b*. Together these results indicate that genes required for expansion and differentiation of NPCs are direct transcriptional targets of Brg1.

3.7. Brg1 and Sall1 bind common target genes in developing kidney

Our model proposes that Sall1 cooperates with SWI/SNF to promote expansion of nephron progenitors. Consistent with this hypothesis, comparing transcriptional profiles between *Sall1*−/− FACS sorted nephron progenitor cells (Basta et al., 2014) and *Brg1* mutant kidneys revealed 167 genes with altered expression in both mutants (Fig. 7A). A prediction of our model is that genomic binding of Sall1 and Brg1 will overlap at target genes that are required for the self-renewal and maintenance of nephron progenitors. To define the genomic targets of Sall1, we performed ChIP-seq on E16.5 wild type kidneys. We found that 15% of Sall1 peaks localized to promoters and 12% to predicted enhancers (Fig. 7B). Comparison of Sall1 and Brg1 binding revealed that 83% of Sall1 bound promoters were also enriched for Brg1 (Fig. 7C). We detected overlapping genomic binding of Sall1 and Brg1 at gene promoters of multiple downregulated progenitor genes, including *Six2*, *Bmp7*, *Fgf9*, *Myc* and *Eya1*, which are required for proliferation and maintenance of nephron progenitor cells (Couillard and Trudel, 2009; Blank et al., 2009; Muthukrishnan et al., 2015; Kobayashi et al., 2008; Barak et al., 2012; Xu et al., 2014) (Fig. 7D–H). We performed gene ontology analysis for target genes that showed both altered mRNA expression in *Sall1* and *Brg1* mutants (Fig. 7I) and whose promoters were bound by both Sall1 and Brg1 (Fig. 7J). Biological processes that were significantly enriched included developmental growth, cell

population proliferation and regulation of programmed cell death, all of which figure prominently in the *Brg1* mutant phenotype. The analysis identified Wnt signaling as a key pathway regulated by Sall1 and Brg1 (Fig. 7I and J). These findings support a model in which Sall1 and SWI/SNF cooperate to promote expansion of nephron progenitor cells mediated at least in part by regulating Wnt activity. Brg1 and Sall1 genomic binding at promoters and putative enhancers was also enriched at genes that are linked to other signaling pathways required for nephron progenitor cell expansion and differentiation, including BMP/SMAD, FGF and MAP kinase (Fig. 7J).

4. Discussion

In order to form a normal complement of nephrons, progenitor cells must undergo a dramatic expansion during kidney development. Self-renewal of nephron progenitors is a tightly regulated process, balanced with differentiation into renal vesicles, the earliest epithelial nephron structure. While our knowledge of individual genes and pathways that control nephron formation has increased substantially, it is not clear how the coordinated action of key factors establishes gene regulatory networks to control nephron progenitor fate. Chromatin-remodeling complexes play an essential role in influencing how cells respond to developmental signals. Through their association with tissue restricted transcription factors, these complexes modulate gene expression to control cell fate, maintaining multi-potency or determining cell lineage. We previously demonstrated that Sall1 associated with NuRD to maintain nephron progenitors by restraining differentiation into renal vesicles (Basta et al., 2017). In the current study, we now show that Sall1 cooperates with a different chromatin remodeler, SWI/SNF, to regulate expansion of nephron progenitor cells.

SWI/SNF is one of four classes of chromatin-remodeling complexes that use the energy of ATP hydrolysis to move or evict nucleosomes, thereby enabling or restricting transcriptional machinery and transcription factor access to DNA to control gene expression. This multi-protein complex plays critical roles in regulating cell proliferation and differentiation during development and its components are among the most frequently mutated genes in cancer, including renal cell carcinoma (Cai et al., 2019; Nargund et al., 2017; Varela et al., 2011); reviewed in (Kadoch, 2019). In humans, mutations in SWI/SNF cause several kidney phenotypes. Coffin-Siris is an intellectual disability syndrome that is due to mutations in several genes that encode for SWI/SNF complex components, including *SMARCA4*, *ARID1A*/*B*, *ARID2*, *SMARCE1*, *SMARCB1* and *DPF2*. In addition to CNS defects, affected individuals have multi-organ defects including the kidney and urinary tract (Vergano et al., 1993, 2018). A variant of Coffin Siris due to autosomal dominant mutations in the N-terminal DNA binding domain of *SMARCB1*, a common core component of BAF and PBAF, causes multiple congenital anomalies including the kidney (Diets et al., 2019). Deletion of *Smarca4*, the gene encoding the SWI/SNF ATPase Brg1 in developing ureteric bud disrupted urothelial cell fate in mice (Weiss et al., 2013). However, the role of SWI/SNF in kidney progenitor cells and nephron formation has not been investigated.

Deletion of *Brg1* in Six2+ nephron progenitor cells resulted in profound growth retardation of the kidney after E14.5. The progressive reduction in Six2+ progenitor cells from E14.5–E17.5 led to secondary reduction in ureteric bud branching, resulting in a nephron deficit.

RNA-seq identified impaired metabolic programming and protein translation at E17.5 in mutant kidneys, but gene expression changes in these cellular processes were not apparent at E14.5, suggesting these were secondary effects. Instead, our data indicate that reductions in three factors, *Bmp7*, *Fgf9* and *Myc* likely accounted for impaired proliferation of nephron progenitor cells in *Brg1* mutant kidneys. mRNA expression of genes encoding each of these factors is significantly reduced at E14.5 and persisted at E16.5. It is likely that the observed changes in metabolic pathways and protein synthesis were secondary to reductions in *Myc*, which regulates these cellular processes [reviewed in (Hsieh et al., 2015); (van Riggelen et al., 2010)]. Previous studies showed that Bmp7, Fgf9 and Myc cooperate to stimulate proliferation of nephron progenitors (Muthukrishnan et al., 2015). Therefore, the reduced expression of these three factors can account for diminished proliferation of nephron progenitor cells in *Brg1* mutants. However, how expression of these genes is regulated in nephron progenitors was not elucidated in these prior studies.

We performed ChIP-seq to define genomic binding of Brg1 in developing kidney. We found that Brg1 bound many promoters of nephron progenitor genes, including *Bmp7*, *Fgf9* and *Myc*. Our studies also revealed that Brg1 likely directly regulated transcription of these genes in cooperation with Sall1. Similar to *Brg1* loss of function, *Sall1* mutant kidneys exhibited reduced cell proliferation but no apoptosis in Six2+ cells prior to onset of the phenotype and reduced expression of *Myc* and *Bmp7* (Basta et al., 2014). While *Fgf9* mRNA was not reduced in *Sall1*−/− kidneys, *Fgf20*, a growth factor that functions redundantly with *Fgf9* in nephron progenitors was significantly downregulated (Barak et al., 2012). Comparing transcriptional profiles of *Brg1* and *Sall1* mutant kidneys identified a large number of genes with altered expression in both mutants, and Sall1 and Brg1 bound promoters of most of these genes. In addition to *Bmp7*, *Myc* and *Fgf9*, these included *Six2*, *Eya1*, *Cited1*, *Meox1*/*2* and *Kif26b*, which are restricted to self-renewing nephron progenitor cells and required for their maintenance. Overall, these studies establish a novel mechanistic link between Sall1, a transcription factor that is essential for kidney development and SWI/SNF.

Myc is a critical regulator of progenitor cell proliferation in developing organs and when dysregulated it promotes neoplasia (Casey et al., 2018; Dang, 2012; Sabo et al., 2014). Conditional deletion of *Myc* in cap mesenchyme using *Bmp7*-Cre resulted in reduced proliferation of nephron progenitors in a restricted developmental window between E14.5 and E17.5 (Couillard and Trudel, 2009). The onset of reduced proliferation and the markedly impaired growth of the *Brg1* mutant kidneys overlapped with this time interval, supporting a role for *Myc* as an important downstream target of Brg1 in developing kidney. However, the degree of renal hypoplasia in *Six2*-Cre $Brg1^{flx/flx}$ is significantly more severe than the *Myc* mutant kidney. One possible explanation is that we also observed a 53% reduction in *N-Myc* expression in *Brg1* mutants. Combined deletion of *Myc* and *N-Myc* in Six2+ cells is more severe than either single mutant indicating functional redundancy. However, the reduction in developing nephron segments at E16.5 (Fig. 5) in *Brg1* mutants is significantly greater than observed in the *Myc*/*N-Myc* double mutant (Pan et al., 2017). The discrepancy between *Myc* and *Brg1* mutant kidney phenotypes cannot be accounted for solely by reduced expansion of Six2+ progenitors. A more likely explanation for the more severe phenotype in Brg1 mutants is that Brg1 is also required to promote differentiation of nephron progenitors. In support of

this idea, we found a 50% reduction in Lef1/NCAM + differentiating structures as early as E14.5 and downregulation of *Lhx1*, *Fgf8*, *Hnfb1*, critical genes that mediate early nephron formation. In addition to its role in promoting proliferation of nephron progenitors via MAP kinase, Bmp7/Smad1/5 signaling promotes differentiation (Blank et al., 2009; Brown et al., 2013, 2015; Muthukrishnan et al., 2015). We propose that reduced Smad1/5 signaling contributed to impaired nephron differentiation in *Brg1* mutant kidneys due to reduced levels of *Bmp7* mRNA and upregulation of *Decorin*, a secreted factor that inhibits Bmp/Smad activity (Fetting et al., 2014). Brg1, but not Sall1 was enriched at promoters of differentiation genes, suggesting that they are direct targets of SWI/SNF. These findings suggest that Sall1 and Brg1 cooperate to expand nephron progenitors. However, Brg1 is also required to promote their differentiation. In contrast, Sall1 through its cooperation with the NuRD chromatin-remodeling complex acts to restrain differentiation, thereby preventing premature depletion of the progenitor cell pool (Basta et al., 2017). Overall, our results highlight Sall1's pivotal role in balancing expansion and differentiation of progenitor cells through its association with distinct chromatin remodeling complexes. However, the molecular mechanisms by which Sall1 coordinates gene expression with these two complexes remains to be elucidated. NuRD and SWI/SNF can have opposing actions on nucleosomes to promote or restrict open chromatin. While NuRD recruits Polycomb (PRC2) to silence some genes, SWI/SNF has the capacity to evict PRC2 and thereby enhance gene transcription in response to signals for self-renewal and differentiation [reviewed in (Bracken et al., 2019)]. Future studies will need to explore mechanisms by which Sall1 coordinates the activity of these chromatin-remodeling complexes to balance expression of genes that expand progenitor cells versus those that promote differentiation into nephrons.

Our studies showed that embryonic kidney expressed components of both main types of SWI/SNF complexes, BAF and PBAF. However, some components displayed dynamic expression during development and certain isoforms (e.g. Baf45 d, Fig. 2B) were enriched in the kidney throughout kidney development. Specific BAF isoforms and unique sub-complexes are required for cardiac development (Hota et al., 2019; Sun et al., 2018; Singh and Archer, 2014). The apparent developmental switch in expression from Baf250a to Baf250b at E17.5 may indicate that Baf250b is required for growth of the kidney between E17.5-P0, when impairment of *Brg1* mutants was most evident. Additional studies are needed to determine if subunit diversity of SWI/SNF complexes regulates unique gene expression profiles and developmental functions in the kidney. In conclusion, we demonstrated that Brg1, the catalytic subunit of SWI/SNF is required for growth of the embryonic kidney by regulating proliferation and differentiation of nephron progenitor cells.

Supplementary Material

Refer to Web version on PubMed Central for supplementary material.

Acknowledgements

These studies were supported by National Institutes of Diabetes, Digestive and Kidney Diseases (DK 098563) and the March of Dimes (6-FY13-127). The authors thank Dr. Dale Dorsett and Ziva Misulovin of the Saint Louis University Genomics Core for assistance with ChIP-seq library preparation and bioinformatics analysis. The authors disclose no competing or financial interests.

References

Ashburner M, Ball CA, Blake JA, Botstein D, Butler H, Cherry JM, et al., 2000 Gene ontology: tool for the unification of biology. The Gene Ontology Consortium. Nat. Genet 25 (1), 25–29. [PubMed: 10802651]

Bagherie-Lachidan M, Reginensi A, Pan Q, Zaveri HP, Scott DA, Blencowe BJ, et al., 2015 Stromal Fat4 acts non-autonomously with Dchs1/2 to restrict the nephron progenitor pool. Development 142 (15), 2564–2573. [PubMed: 26116661]

Barak H, Huh SH, Chen S, Jeanpierre C, Martinovic J, Parisot M, et al., 2012 FGF9 and FGF20 maintain the stemness of nephron progenitors in mice and man. Dev. Cell 22 (6), 1191–1207. [PubMed: 22698282]

Barker DJ, Shiell AW, Barker ME, Law CM, 2000 Growth in utero and blood pressure levels in the next generation. J. Hypertens 18 (7), 843–846. [PubMed: 10930180]

Basta JM, Robbins L, Kiefer SM, Dorsett D, Rauchman M, 2014 Sall1 balances self-renewal and differentiation of renal progenitor cells. Development 141 (5), 1047–1058. [PubMed: 24550112]

Basta JM, Robbins L, Denner DR, Kolar GR, Rauchman M, 2017 A Sall1-NuRD interaction regulates multipotent nephron progenitors and is required for loop of Henle formation. Development 144 (17), 3080–3094. [PubMed: 28760814]

Blank U, Brown A, Adams DC, Karolak MJ, Oxburgh L, 2009 BMP7 promotes proliferation of nephron progenitor cells via a JNK-dependent mechanism. Development 136 (21), 3557–3566. [PubMed: 19793891]

Bozal-Basterra L, Martin-Ruiz I, Pirone L, Liang Y, Sigurethsson JO, Gonzalez-Santamarta M, et al., 2018 Truncated SALL1 impedes primary cilia function in townes-brocks syndrome. Am. J. Hum. Genet 102 (2), 249–265. [PubMed: 29395072]

Bracken AP, Brien GL, Verrijzer CP, 2019 Dangerous liaisons: interplay between SWI/SNF, NuRD, and Polycomb in chromatin regulation and cancer. Genes Dev. 33 (15–16), 936–959. [PubMed: 31123059]

Brown AC, Blank U, Adams DC, Karolak MJ, Fetting JL, Hill BL, et al., 2011 Isolation and culture of cells from the nephrogenic zone of the embryonic mouse kidney. JoVE (50).

Brown AC, Muthukrishnan SD, Guay JA, Adams DC, Schafer DA, Fetting JL, et al., 2013 Role for compartmentalization in nephron progenitor differentiation. Proc. Natl. Acad. Sci. U. S. A 110 (12), 4640–4645. [PubMed: 23487745]

Brown AC, Muthukrishnan SD, Oxburgh L, 2015 A synthetic niche for nephron progenitor cells. Dev. Cell 34 (2), 229–241. [PubMed: 26190145]

Cai W, Su L, Liao L, Liu ZZ, Langbein L, Dulaimi E, et al., 2019 PBRM1 acts as a p53 lysine-acetylation reader to suppress renal tumor growth. Nat. Commun 10 (1), 5800. [PubMed: 31863007]

Casey SC, Baylot V, Felsher DW, 2018 The MYC oncogene is a global regulator of the immune response. Blood 131 (18), 2007–2015. [PubMed: 29514782]

Cebrian C, Asai N, D'Agati V, Costantini F, 2014 The number of fetal nephron progenitor cells limits ureteric branching and adult nephron endowment. Cell Rep. 7 (1), 127–137. [PubMed: 24656820]

Couillard M, Trudel M, 2009 C-myc as a modulator of renal stem/progenitor cell population. Dev. Dynam 238 (2), 405–414.

Dang CV, 2012 MYC on the path to cancer. Cell 149 (1), 22–35. [PubMed: 22464321]

Denner DR, Rauchman M, 2013 Mi-2/NuRD is required in renal progenitor cells during embryonic kidney development. Dev. Biol 375 (2), 105–116. [PubMed: 23201013]

Diets IJ, Prescott T, Champaigne NL, Mancini GMS, Krossnes B, Fric R, et al., 2019 A recurrent de novo missense pathogenic variant in SMARCB1 causes severe intellectual disability and choroid plexus hyperplasia with resultant hydrocephalus. Genet. Med 21 (3), 572–579. [PubMed: 29907796]

Dorsett D, Misulovin Z, 2017 Measuring sister chromatid cohesion protein genome occupancy in Drosophila melanogaster by ChIP-seq. Methods Mol. Biol 1515, 125–139. [PubMed: 27797077]

Fergelot P, Van Belzen M, Van Gils J, Afenjar A, Armour CM, Arveiler B, et al., 2016 Phenotype and genotype in 52 patients with Rubinstein-Taybi syndrome caused by EP300 mutations. Am. J. Med. Genet 170 (12), 3069–3082. [PubMed: 27648933]

Fetting JL, Guay JA, Karolak MJ, Iozzo RV, Adams DC, Maridas DE, et al., 2014 FOXD1 promotes nephron progenitor differentiation by repressing decorin in the embryonic kidney. Development 141 (1), 17–27. [PubMed: 24284212]

Gatchalian J, Malik S, Ho J, Lee DS, Kelso TWR, Shokhirev MN, et al., 2018 A non-canonical BRD9-containing BAF chromatin remodeling complex regulates naive pluripotency in mouse embryonic stem cells. Nat. Commun 9 (1), 5139. [PubMed: 30510198]

Hartman HA, Lai HL, Patterson LT, 2007 Cessation of renal morphogenesis in mice. Dev. Biol 310 (2), 379–387. [PubMed: 17826763]

Hota SK, Bruneau BG, 2016 ATP-dependent chromatin remodeling during mammalian development. Development 143 (16), 2882–2897. [PubMed: 27531948]

Hota SK, Johnson JR, Verschueren E, Thomas R, Blotnick AM, Zhu Y, et al., 2019 Dynamic BAF chromatin remodeling complex subunit inclusion promotes temporally distinct gene expression programs in cardiogenesis. Development 146 (19).

Hoy WE, Hughson MD, Singh GR, Douglas-Denton R, Bertram JF, 2006 Reduced nephron number and glomerulomegaly in Australian Aborigines: a group at high risk for renal disease and hypertension. Kidney Int. 70 (1), 104–110. [PubMed: 16723986]

Hsieh AL, Walton ZE, Altman BJ, Stine ZE, Dang CV, 2015 MYC and metabolism on the path to cancer. Semin. Cell Dev. Biol 43, 11–21. [PubMed: 26277543]

Huang da W., Sherman BT, Lempicki RA, 2009 Systematic and integrative analysis of large gene lists using DAVID bioinformatics resources. Nat. Protoc 4 (1), 44–57. [PubMed: 19131956]

Huang da W., Sherman BT, Lempicki RA, 2009 Bioinformatics enrichment tools: paths toward the comprehensive functional analysis of large gene lists. Nucleic Acids Res. 37 (1), 1–13. [PubMed: 19033363]

Kadoch C, 2019 Diverse compositions and functions of chromatin remodeling machines in cancer. Sci. Transl. Med 11 (501).

Kanda S, Tanigawa S, Ohmori T, Taguchi A, Kudo K, Suzuki Y, et al., 2014 Sall1 maintains nephron progenitors and nascent nephrons by acting as both an activator and a repressor. J. Am. Soc. Nephrol 25 (11), 2584–2595. [PubMed: 24744442]

Keller G, Zimmer G, Mall G, Ritz E, Amann K, 2003 Nephron number in patients with primary hypertension. N. Engl. J. Med 348 (2), 101–108. [PubMed: 12519920]

Kiefer SM, Robbins L, Rauchman M, 2012 Conditional expression of Wnt9b in Six2-positive cells disrupts stomach and kidney function. PloS One 7 (8), e43098. [PubMed: 22912798]

Kobayashi A, Valerius MT, Mugford JW, Carroll TJ, Self M, Oliver G, et al., 2008 Six2 defines and regulates a multipotent self-renewing nephron progenitor population throughout mammalian kidney development. Cell Stem Cell 3 (2), 169–181. [PubMed: 18682239]

Lauberth SM, Rauchman M, 2006 A conserved 12-amino acid motif in Sall1 recruits the nucleosome remodeling and deacetylase corepressor complex. J. Biol. Chem 281 (33), 23922–23931. [PubMed: 16707490]

Lauberth SM, Bilyeu AC, Firulli BA, Kroll KL, Rauchman M, 2007 A phosphomimetic mutation in the Sall1 repression motif disrupts recruitment of the nucleosome remodeling and deacetylase complex and repression of Gbx2. J. Biol. Chem 282 (48), 34858–34868. [PubMed: 17895244]

Legendre M, Abadie V, Attie-Bitach T, Philip N, Busa T, Bonneau D, et al., 2017 Phenotype and genotype analysis of a French cohort of 119 patients with CHARGE syndrome. Am J Med Genet C Semin Med Genet 175 (4), 417–430. [PubMed: 29178447]

Li SY, Park J, Guan Y, Chung K, Shrestha R, Palmer MB, et al., 2019 DNMT1 in Six2 progenitor cells is essential for transposable element silencing and kidney development. J. Am. Soc. Nephrol 30 (4), 594–609. [PubMed: 30850438]

Muthukrishnan SD, Yang X, Friesel R, Oxburgh L, 2015 Concurrent BMP7 and FGF9 signalling governs AP-1 function to promote self-renewal of nephron progenitor cells. Nat. Commun 6, 10027. [PubMed: 26634297]

Nagarajan S, Rao SV, Sutton J, Cheeseman D, Dunn S, Papachristou EK, et al., 2020 ARID1A influences HDAC1/BRD4 activity, intrinsic proliferative capacity and breast cancer treatment response. Nat. Genet 52 (2), 187–197. [PubMed: 31913353]

Nargund AM, Pham CG, Dong Y, Wang PI, Osmangeyoglu HU, Xie Y, et al., 2017 The SWI/SNF protein PBRM1 restrains VHL-loss-driven clear cell renal cell carcinoma. Cell Rep. 18 (12), 2893–2906. [PubMed: 28329682]

Oliveros JC. Venny. An Interactive Tool for Comparing Lists with Venn's Diagrams. http://bioinfogp.cnb.csic.es/tools/venny/index.html. 2007-2015.

Pan X, Karner CM, Carroll TJ, 2017 Myc cooperates with beta-catenin to drive gene expression in nephron progenitor cells. Development 144 (22), 4173–4182. [PubMed: 28993399]

Patel SR, Bhumbra SS, Paknikar RS, Dressler GR, 2012 Epigenetic mechanisms of Groucho/Grg/TLE mediated transcriptional repression. Mol. Cell 45 (2), 185–195. [PubMed: 22169276]

Porter EG, Dykhuizen EC, 2017 Individual bromodomains of polybromo-1 contribute to chromatin association and tumor suppression in clear cell renal carcinoma. J. Biol. Chem 292 (7), 2601–2610. [PubMed: 28053089]

Quinlan AR, Hall IM, 2010 BEDTools: a flexible suite of utilities for comparing genomic features. Bioinformatics 26 (6), 841–842. [PubMed: 20110278]

Ruijtenberg S, van den Heuvel S, 2015 G1/S inhibitors and the SWI/SNF complex control cell-cycle exit during muscle differentiation. Cell 162 (2), 300–313. [PubMed: 26144318]

Rumballe BA, Georgas KM, Combes AN, Ju AL, Gilbert T, Little MH, 2011 Nephron formation adopts a novel spatial topology at cessation of nephrogenesis. Dev. Biol 360 (1), 110–122. [PubMed: 21963425]

Sabo A, Kress TR, Pelizzola M, de Pretis S, Gorski MM, Tesi A, et al., 2014 Selective transcriptional regulation by Myc in cellular growth control and lymphomagenesis. Nature 511 (7510), 488–492. [PubMed: 25043028]

Singh AP, Archer TK, 2014 Analysis of the SWI/SNF chromatin-remodeling complex during early heart development and BAF250a repression cardiac gene transcription during P19 cell differentiation. Nucleic Acids Res. 42 (5), 2958–2975. [PubMed: 24335282]

Singh AP, Foley JF, Rubino M, Boyle MC, Tandon A, Shah R, et al., 2016 Brg1 enables rapid growth of the early embryo by suppressing genes that regulate apoptosis and cell growth arrest. Mol. Cell Biol 36 (15), 1990–2010. [PubMed: 27185875]

Singh AP, Foley J, Tandon A, Phadke D, Karimi Kinyamu H, Archer TK, 2017 A role for BRG1 in the regulation of genes required for development of the lymphatic system. Oncotarget 8 (33), 54925–54938. [PubMed: 28903392]

Stojanova A, Tu WB, Ponzielli R, Kotlyar M, Chan PK, Boutros PC, et al., 2016 MYC interaction with the tumor suppressive SWI/SNF complex member INI1 regulates transcription and cellular transformation. Cell Cycle 15 (13), 1693–1705. [PubMed: 27267444]

Sun X, Hota SK, Zhou YQ, Novak S, Miguel-Perez D, Christodoulou D, et al., 2018 Cardiac-enriched BAF chromatin-remodeling complex subunit Baf60c regulates gene expression programs essential for heart development and function. Biol Open 7 (1).

The Gene Ontology, C., 2019 The gene ontology resource: 20 years and still GOing strong. Nucleic Acids Res. 47 (D1), D330–D338. [PubMed: 30395331]

van Riggelen J, Yetil A, Felsher DW, 2010 MYC as a regulator of ribosome biogenesis and protein synthesis. Nat. Rev. Canc 10 (4), 301–309.

Varela I, Tarpey P, Raine K, Huang D, Ong CK, Stephens P, et al., 2011 Exome sequencing identifies frequent mutation of the SWI/SNF complex gene PBRM1 in renal carcinoma. Nature 469 (7331), 539–542. [PubMed: 21248752]

Vergano SA, van der Sluijs PJ, Santen G, 1993 ARID1B-Related disorder In: Adam MP, Ardinger HH, Pagon RA, Wallace SE, Bean LJH, Stephens K, et al. (Eds.), GeneReviews((R)). Seattle (WA.

Vergano S, Santen G, Wieczorek D, Wollnik B, Matsumoto N, Deardorff M, 2018 In: Ardinger HH, Pagon RA, et al. (Eds.), Gene Reviews Adam MP. University of Washington, Seattle, WA Seattle, WA.

Wanner N, Vornweg J, Combes A, Wilson S, Plappert J, Rafflenbeul G, et al., 2019 DNA methyltransferase 1 controls nephron progenitor cell renewal and differentiation. J. Am. Soc. Nephrol 30 (1), 63–78. [PubMed: 30518531]

Weiss RM, Guo S, Shan A, Shi H, Romano RA, Sinha S, et al., 2013 Brg1 determines urothelial cell fate during ureter development. J. Am. Soc. Nephrol 24 (4), 618–626. [PubMed: 23449535]

Xu J, Wong EY, Cheng C, Li J, Sharkar MT, Xu CY, et al., 2014 Eya1 interacts with Six2 and Myc to regulate expansion of the nephron progenitor pool during nephrogenesis. Dev. Cell 31 (4), 434–447. [PubMed: 25458011]

Zhang L, Ettou S, Khalid M, Taglienti M, Jain D, Jung YL, et al., 2018 EED, a member of the polycomb group, is required for nephron differentiation and the maintenance of nephron progenitor cells. Development 145 (14).

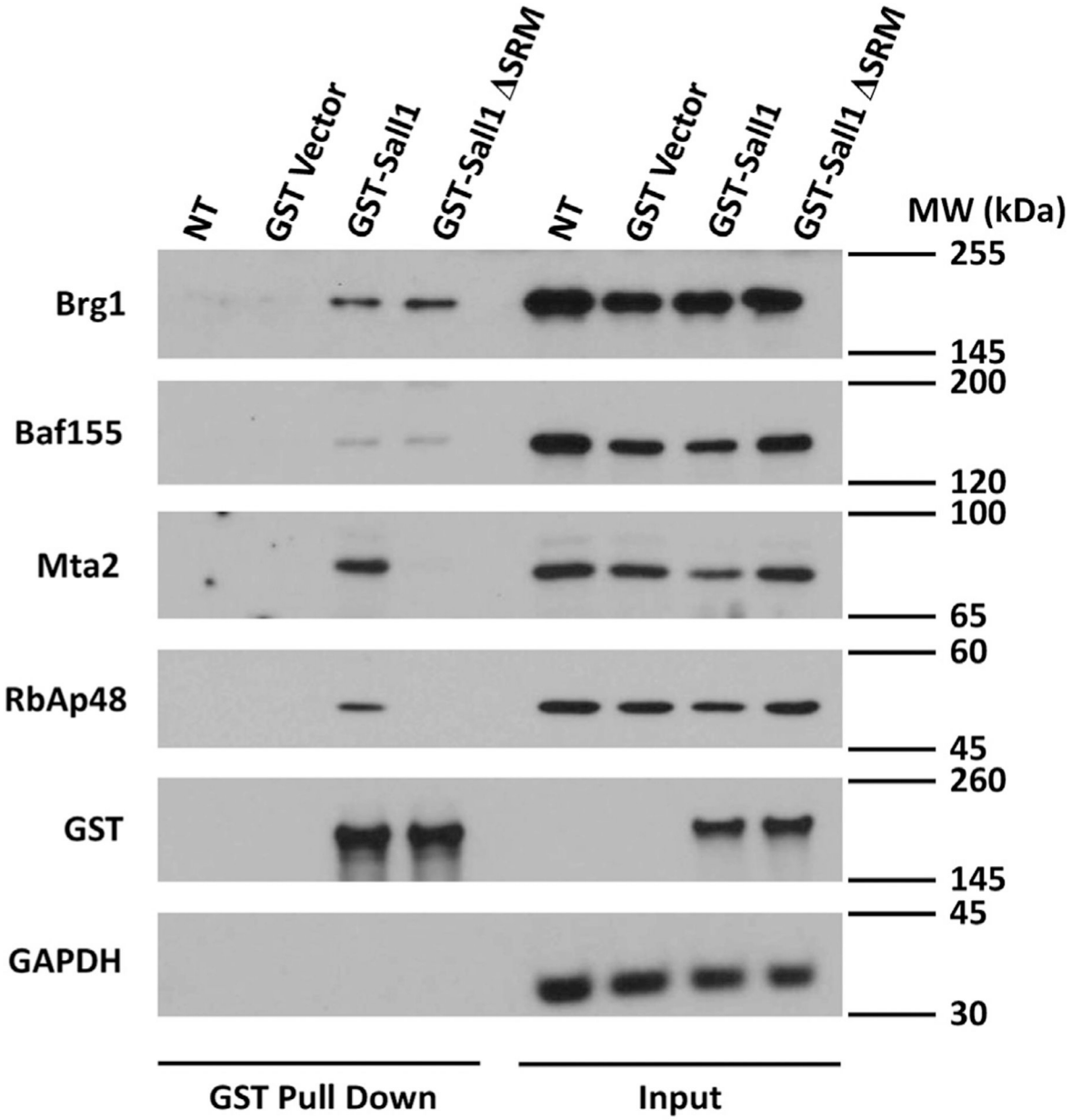

Fig. 1.

Sall1 associates with SWI/SNF subunits. GST-fusion constructs of Sall1 wild type and Sall1-ΔSRM were expressed in COS-1 cells, which express NuRD and SWI-SNF complex components endogenously but do not express Sall1 or other Sall1 family members (Sall2–4). Cell lysates were precipitated with glutathione sepharose (GST) and analyzed by western blot using antibodies to Brg1, Baf155, RbAp48, Mta2, GST, and Gapdh. Sall1, but not Sall1-ΔSRM pulled down NuRD components Mta2 and RbAp48. SWI/SNF subunits Brg1 and Baf 155 (Smarcc1) interacted with wild type Sall1 and the mutant Sall1-ΔSRM that disrupts the association with NuRD, n = 2.

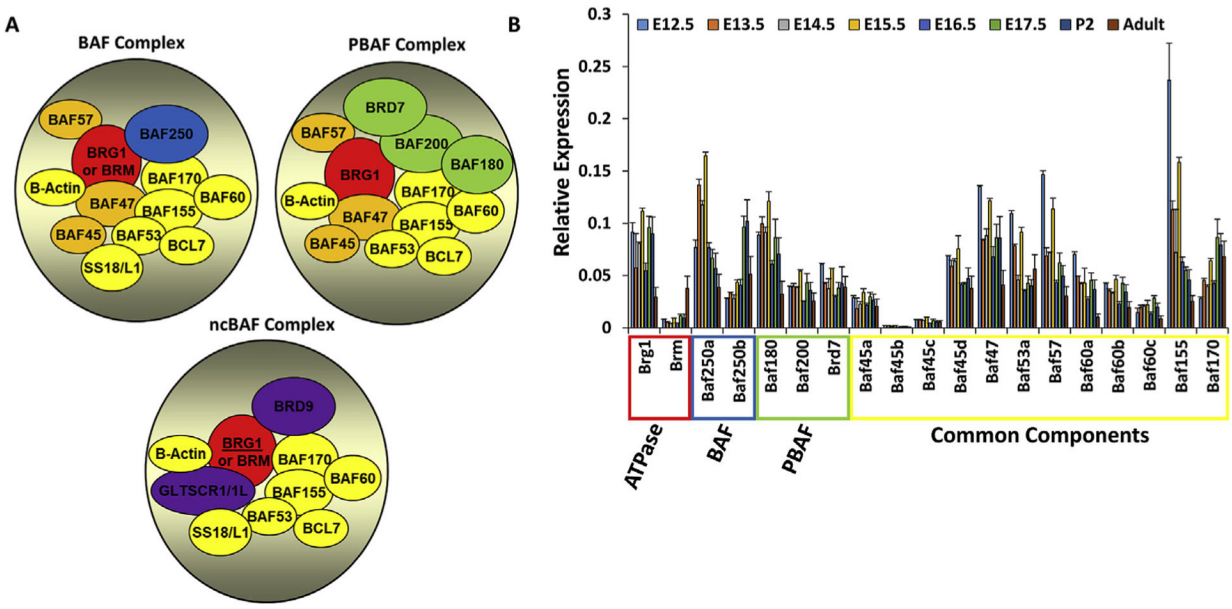

Fig. 2.

Developmental genes expression of SWI/SNF subunits. A. Schematic representation of the two main SWI/SNF complexes, BAF, PBAF, and the non-canonical complex ncBAF. B. Temporal expression profile of genes encoding SWI/SNF subunit in developing and adult kidney. mRNA expression was determined by real time RT-PCR. Relative expression was normalized to *Gapdh*.

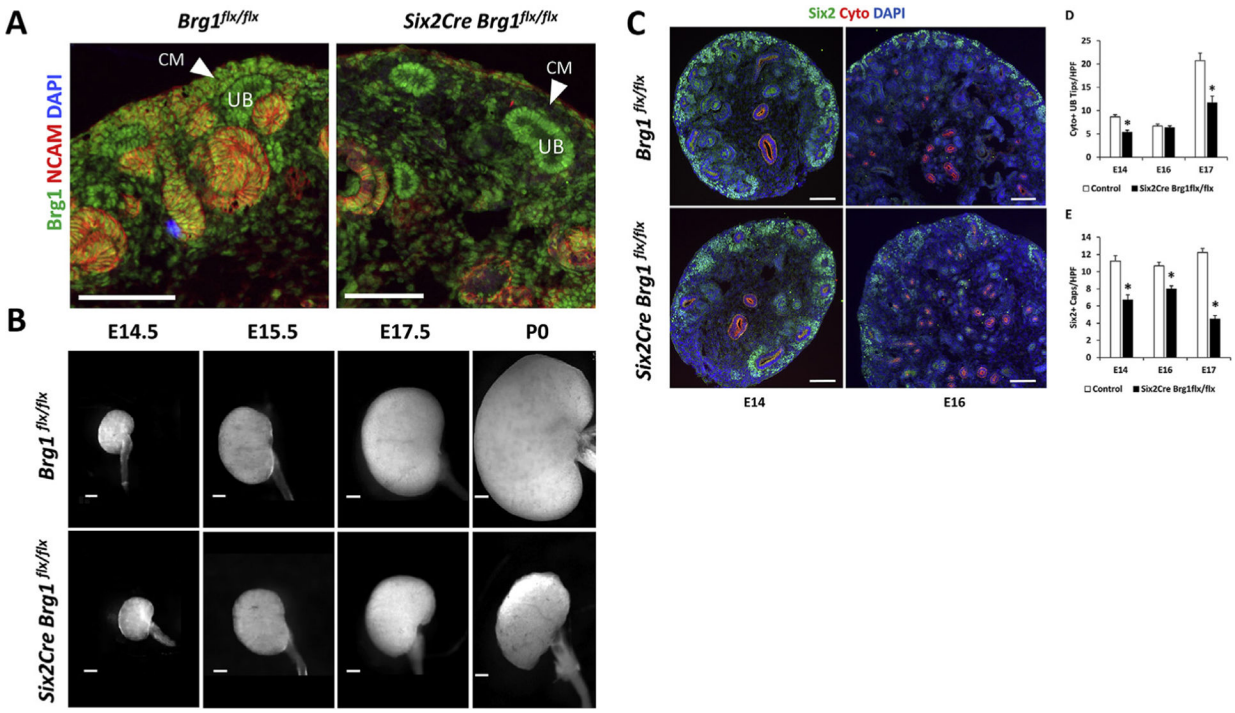

Fig. 3.

Genetic deletion of *Brg1* in Six2 + cells results in renal hypoplasia. A. Brg1 protein is expressed cap mesenchyme (CM, nephron progenitors), stroma, differentiating nephron structures and ureteric bud (UB) in E14.5 wild type kidneys. In E14.5 *Six2*-Cre, $Brg1^{flx/flx}$, Brg1 protein expression is lost in CM and its derivatives in developing nephrons, but retained in stroma and UB, scale bar = 100 μm. B. At E14.5–15.5, a minority of *Six2*-Cre, $Brg1^{flx/flx}$ kidneys show a modest reduction in size. After E15.5, growth of *Six2*-Cre, $Brg1^{flx/flx}$ kidneys significantly lags behind kidneys from control littermates, scale bar = 100 μm. C–E. Quantification of UB tips and Six2+ caps at different developmental stages in wild type and mutant kidney. Cytokeratin + UB tips were reduced in the mutant at E14.5 and E17.5, but not at E16.5. Six2+ caps were significantly diminished at all embryonic stages tested. Representative images of E14.5 and E16.5 kidney used for counting UB tips and caps, stained for cytokeratin, Six2 and DAPI. n = 3 for each stage and genotype, *$p < 0.05$. Statistical analysis was carried out by unpaired two-tailed *t*-test. Scale bar = 100 μm.

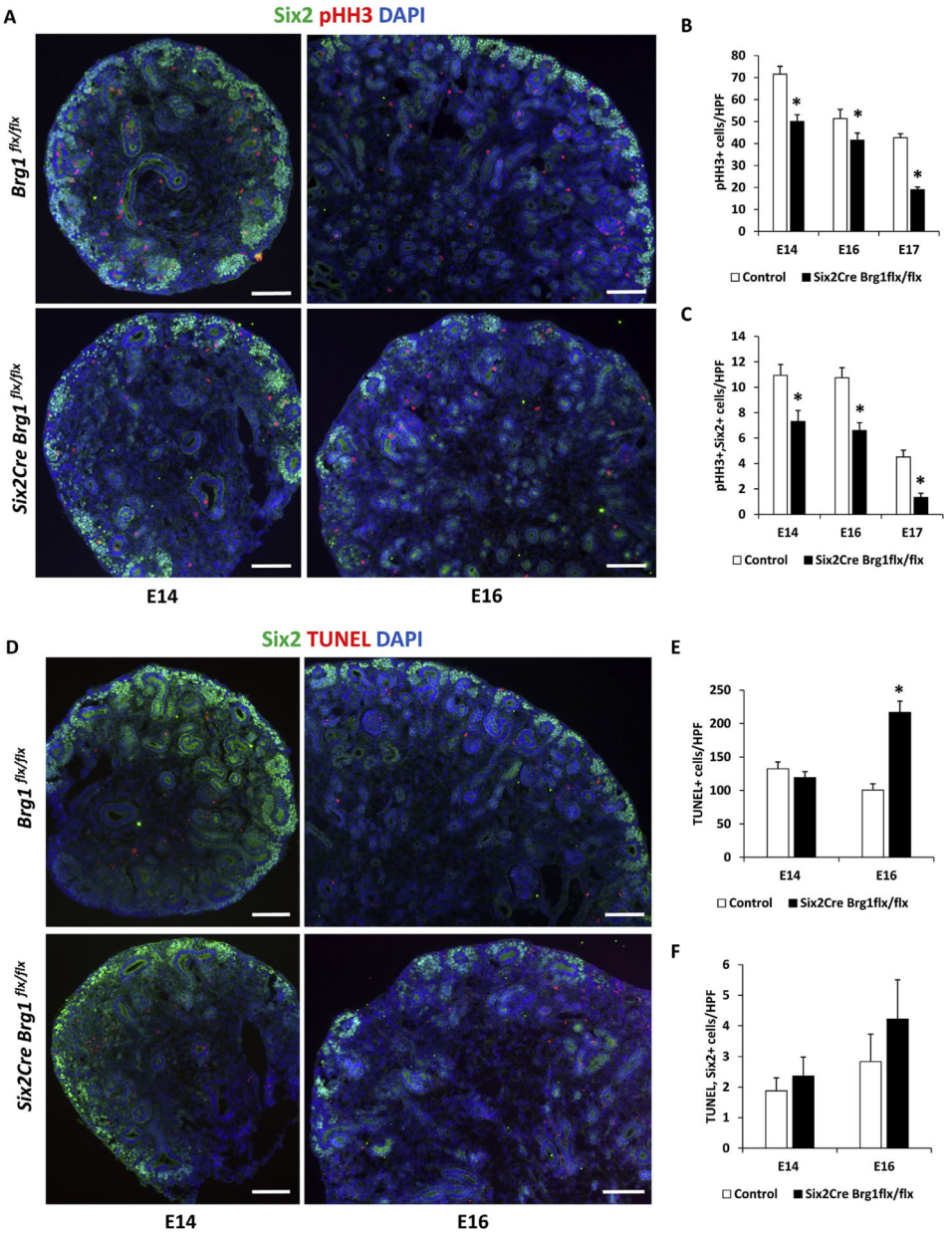

Fig. 4.

Reduced cell proliferation not apoptosis leads to depletion of nephron progenitor cells in *Six2*-Cre, *Brg1*$^{flx/flx}$ mutants. A–C. Quantification of mitotic cells by counting pHH3+, Six2+ cells per high-powered field (HPF). Total mitotic (B) and mitotic Six2+ progenitor cells (C) is reduced at E14.5, E16.5 and E17.5 in mutant kidneys. Representative images of E14 and E16 kidney used for quantification of mitotic cells (A), stained for pHH3, Six2, and DAPI are shown. D–F. Quantification of the number of TUNEL + cells per HPF. Total TUNEL + cells are increased in the mutant at E16.5 but not E14.5. However, quantification of TUNEL+, Six2+ cells/HPF did not reveal a significant increase in apoptosis in mutant nephron progenitors at E14.5 or E16.5 (F). Representative images of E14.5 and E16.5 kidney used for quantification of TUNEL+, Six2+ cells are shown (D). n = 4 for each stage

and genotype. Data were analyzed by unpaired two tailed *t*-test. *p < 0.05. Scale bar = 100 μm.

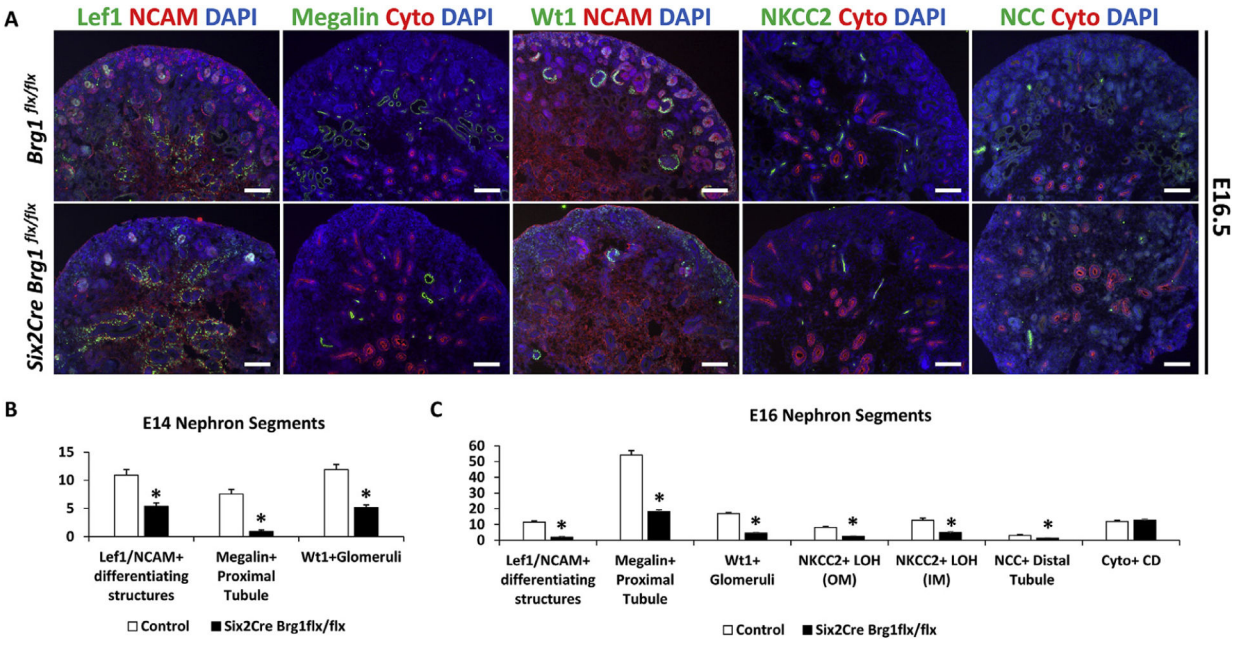

Fig. 5.

Nephron differentiation is impaired in *Six2*-Cre, *Brg1*$^{flx/flx}$ mutants. A. Representative images from E16.5 kidney immunostained for markers of renal vesicles (Lef1/NCAM), proximal tubules (Megalin), glomeruli (Wt1), loops of Henle (NKCC2), distal tubule (NCC) and collecting ducts (cytokeratin). Scale bar = 100 μm. B. Quantitation of renal vesicles and terminally differentiating nephron segments. Graphs represent the average number of segments/HPF (B, C). At E14.5 there is a 50% reduction in Lef1/NCAM + differentiating structures and Wt1+ glomeruli; Meglalin + proximal tubules were reduced by 87% at E14.5. At E16.5, the number of renal vesicles and all nephron segments except collecting ducts is reduced by > 50%. n = 4 for each stage and genotype, *$p < 0.05$ by unpaired two tailed *t*-test.

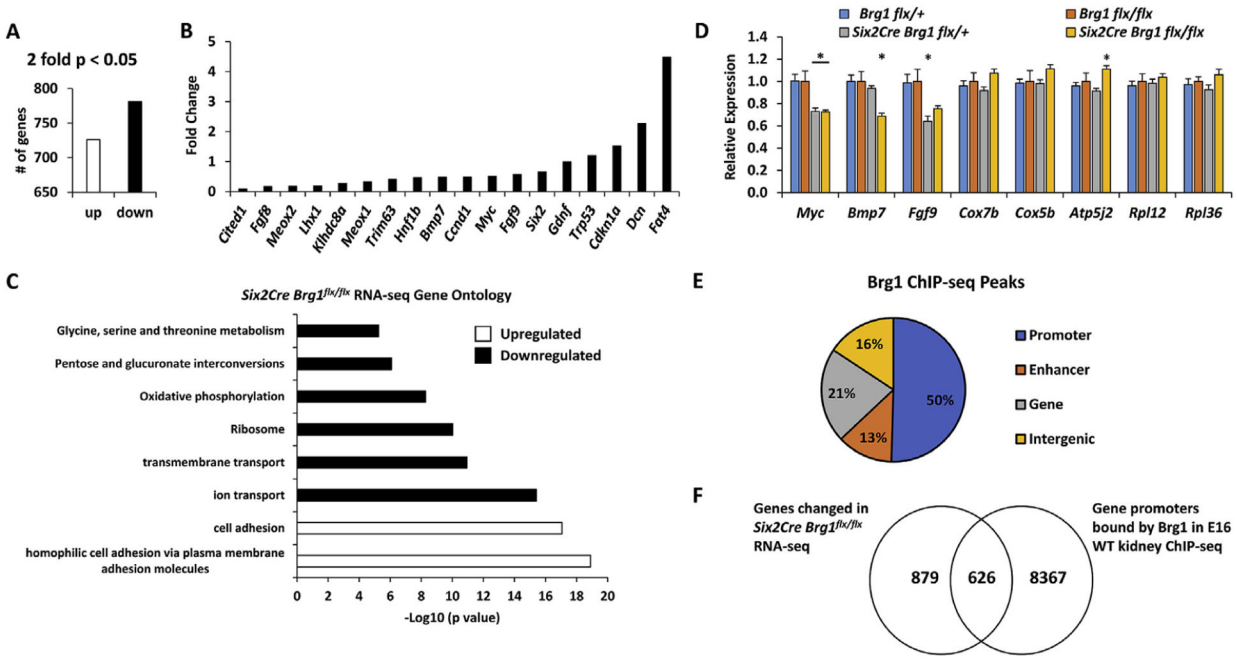

Fig. 6.

Identification of Brg1 target genes in the developing kidney. A. RNA was isolated from E17.5 embryonic *Brg1*$^{flx/flx}$ and *Six2*-Cre, *Brg1*$^{flx/flx}$ kidneys. RNA-seq was performed to compare transcriptional profiles of control and mutant kidneys. 781 genes were downregulated and 726 upregulated in the mutant compared with control kidneys using a threshold of 2-fold change in mRNA expression. n = 3 from each genotype. B. Graph depicting progenitor and differentiation genes that showed altered expression in the mutant kidney by RNA-seq. C. Gene ontology analysis revealed enrichment for metabolic pathways and ribosomal biogenesis among downregulated genes, and cell adhesion for genes upregulated in the mutant kidney at E17.5. D. Oxidative phosphorylation and ribosomal genes that showed the most significant changes at E17.5 were not altered when tested by real time RT-PCR at E14.5. However, genes required to maintain nephron progenitors, *Bmp7*, *Fgf9*, *Myc* were significantly reduced at E14.5 (*Brg1flx*/+ n = 4, *Brg1*$^{flx/flx}$ n = 4, *Six2-Cre Brg1*$^{flx/+}$ n = 6, *Six2-Cre Brg1*$^{flx/flx}$ n = 6, data analyzed by one-way ANOVA followed by multiple-group comparison analysis with Tukey correction, $p < 0.05$). E. Chip-seq was performed to define genomic binding of Brg1 in E16.5 wild type kidney. Brg1 binding was most highly enriched at gene promoters. F. Brg1 bound 42% (626/1505) of genes that showed altered expression by RNA seq in *Six2*-Cre, *Brg1*$^{flx/flx}$ kidneys.

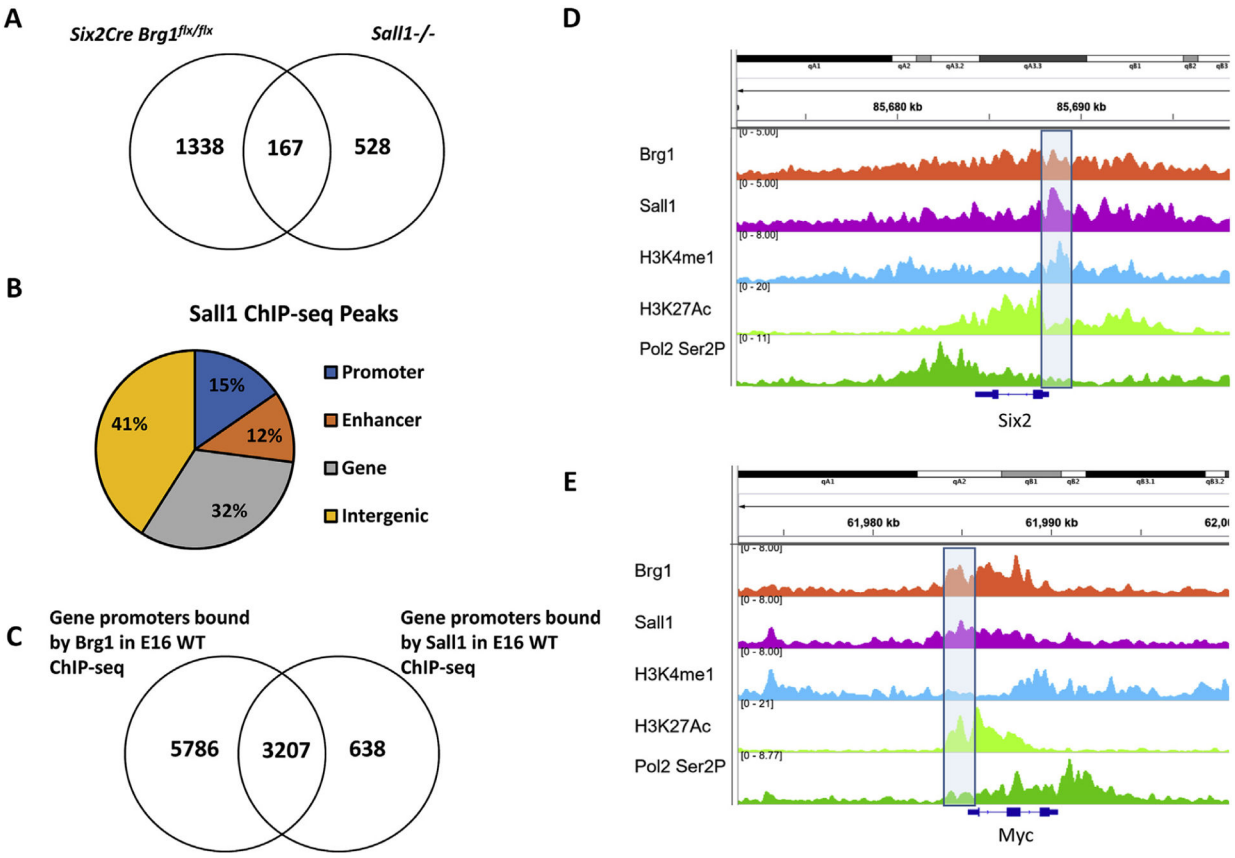

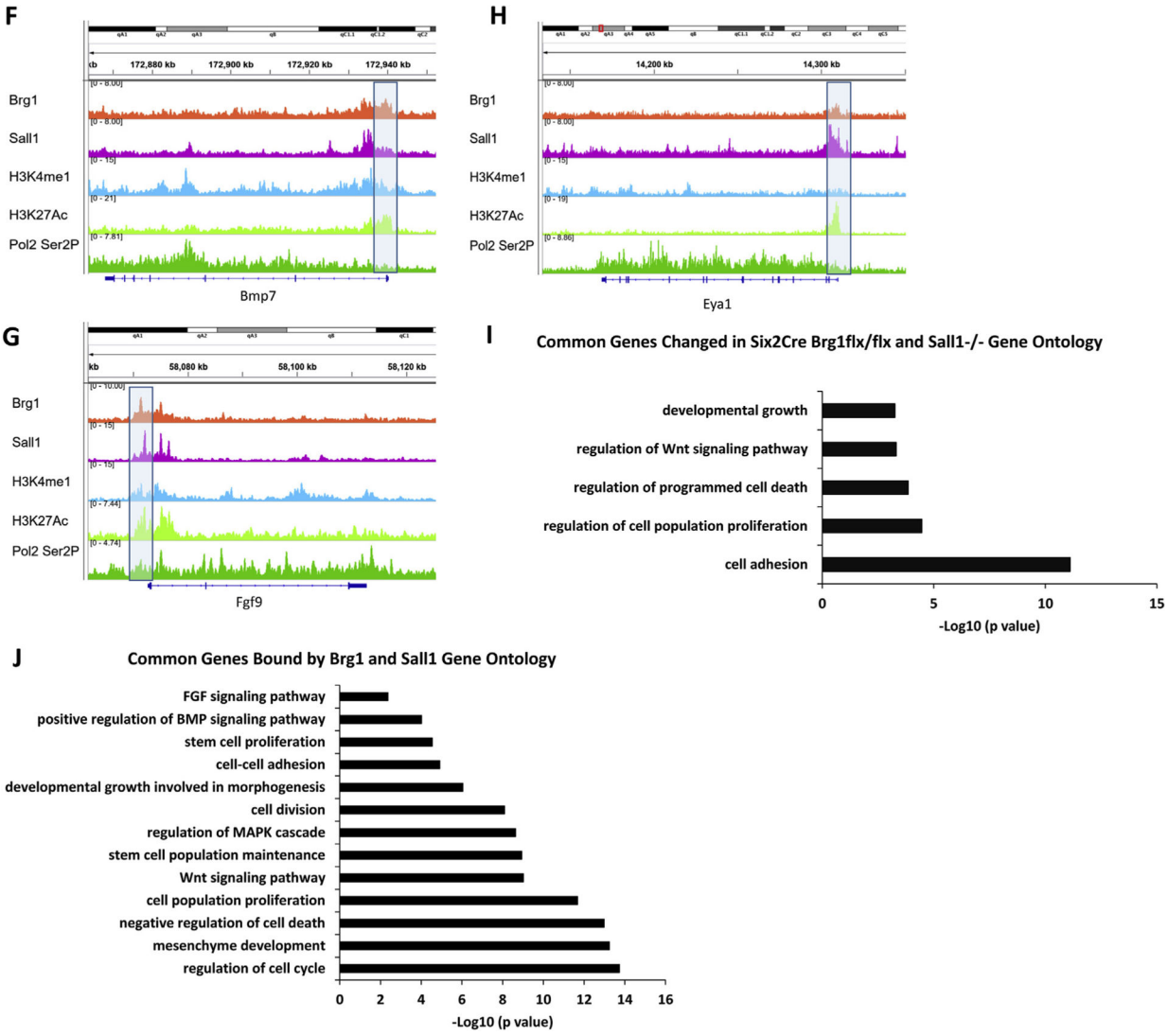

Fig. 7.

Sall1 and Brg1 bind common promoters of nephron progenitor genes. A. Venn diagram showing genes with altered expression in *Six2-Cre Brg1*$^{flx/flx}$ embryonic kidney and *Sall1*−/− nephron progenitor cells. B. Pie chart showing distribution of Sall1 genomic binding. C. Venn diagram showing common promoters bound by both Sall1 and Brg1. D–H. ChIP-seq tracks for Sall1, Brg1, H3K4me1, H3K27ac and RNA Pol II in E16.5 whole kidney showing promoter binding of Sall1 and Brg1 at nephron progenitor genes *Six2*, *Myc*, *Bmp7*, *Fgf9*, *Eya1*. I, Gene ontology for genes with altered expression in *Six2-Cre Brg1*$^{flx/flx}$ and *Sall1*−/− kidneys. J. Gene ontology for promoters of genes bound by both Sall1 and Brg1.

Table 1

Stage	n	*Brg1flx/flx*	*Six2Cre, Brg1flx/flx*
E13, 14	41	23, normal	2/18 hypoplastic
E15, 16	60	37, normal	4/23 hypoplastic
E17, P0	37	23, normal	14/14 hypoplastic